International Journal of Chemical Studies

P-ISSN: 2349–8528
E-ISSN: 2321–4902
IJCS 2018; 6(5): 111-117

Received: 01-07-2018
Accepted: 05-08-2018

**Sanjeev Verma**
Catalysis Laboratory, Indian Institute of Technology, Banaras Hindu University, Varanasi, Uttar Pradesh, India

**Bhawana Verma**
Catalysis Laboratory, Indian Institute of Technology, Banaras Hindu University, Varanasi, Uttar Pradesh, India

**Correspondence**
**Sanjeev Verma**
Catalysis Laboratory, Indian Institute of Technology, Banaras Hindu University, Varanasi, Uttar Pradesh, India

# Synthesis of sulfur/phosphorous-doped graphene aerogel as a modified super capacitor electrode

**Sanjeev Verma and Bhawana Verma**

**Abstract**
This paper reports the synthesis of Sulfur/Phosphorous doped Graphene aerogel from reduced Graphene sheets and characterized by scanning electron microscopy (SEM), Fourier transform infrared spectroscopy (FTIR) and X-ray diffraction (XRD) data. From the comparative study between Sulfur doped Graphene aerogel and Phosphorous doped Graphene aerogel as super capacitor, it has been found that the specific capacitance of Sulfur doped Graphene aerogel was found to be 750.75 $Fg^{-1}$ and 360.75 $Fg^{-1}$ for phosphorous doped Graphene aerogel respectively at scan rate of 20 $mVs^{-1}$. Data obtained from the specific capacitance clearly indicated that Sulfur doped Graphene aerogel showed a high potential for the use in low cost energy storage devices than phosphorous doped Graphene aerogel.

**Keywords:** graphene, super capacitor, sulfur, phosphorous and specific capacitance

## Introduction
Energy is fundamental source for humankind. Requirement of energy for the variable sources are expected to increase continuously due to population growth and changing lifestyles **[1]**. Researchers have accepts these challenges to develop energy storage devices with long life time batteries and capacitors that can overcome problem to keep up with the current rate of electronic component evolution for a number of years. The electrochemical capacitors are promising and efficient energy storage devices because they can store and release energy quickly [2]. Unlike batteries, when these are integrated with microelectronic devices which increase the duration capacity for very long periods of time without losing their energy storage capacity [3].

For the resolution of this problem researcher designed hybridized lithium-ion battery, which fill the gap between energy and power demand, a key requirement for hybrid electric vehicles and power backup for portable electronics [4]. Keep in mind this idea, Graphene leads to new possibilities for energy storage, with high charge and discharge rates devices [5]. 2D structure of graphene makes it the thinnest material in the known universe. Structure of graphene improves charging and discharging characteristic [6-7]. Graphene is undoubtedly emerging as one of the most promising nano materials because of its unique properties, which opens a way for its exploitation in a wide spectrum of applications ranging from electronics to optics, sensors, and bio-devices. Because of this reason nanotechnology researchers are so excited to develop new class of materials with novel electronic, optical and mechanical properties through modifications [8].

The zero bands gap of graphene weakness its application. So, the chemical doping of graphene of GO sheets, improve its electronic environment and its intrinsic properties **[9]**. Heteroatom-doped graphitic frameworks have received great attention in energy research, since doping endows graphitic structures with a wide spectrum of properties, especially critical for electrochemical super capacitors, which tend to complement or compete with the current lithium ion battery technology [10]. Graphene is a zero band gap material, where the conduction and valence bands touch each other at a point called Dirac point but don't overlap each other, so that graphene remains a semiconductor and not a purely conductor, but after doping the band gap between the conduction and valence bands will be wider, thus it shows the conductive nature [11]. After the doping in graphene oxide, its power density storage energy will get enhanced [12-13].

## Material and Methods

### Synthesis of exfoliated graphene oxide

Graphene oxide is prepared by modified Hummer's method [14]. The graphene oxide was prepared by taking 1 g of exfoliated graphite flakes and suspended in 23 ml of concentrated sulfuric acid containing 50 mg of sodium nitrate. While maintaining vigorous agitation, 3 g of $KMnO_4$ was added to the suspension in a controlled manner and the temperature of the bath was maintained below $20^0$C using an ice bath. After the addition of the $KMnO_4$, the temperature of the suspension was brought to $35^0$C, where it was maintained for 30 minutes. A brownish grey paste was obtained after 20 minutes. After that 50 ml of water was slowly added to this mixture which caused violent effervescence and the temperature rise to $98^0$C. The diluted suspension, brown in color was maintained at this temperature for 15 minutes, further diluted with warm water, and treated with 3% H2O2 to convert the residual permanganate and manganese dioxide to manganese sulfate. The suspension turned bright yellow after treatment with the peroxide. After removing the supernatant, the residue was washed with water and finally dried in an air oven overnight at $110^0$C. The sample was labeled as EGO.

The obtained yellowish brown exfoliated graphene oxide was suspended in water and sonicated for 15 minutes using an ULTRASONICATOR (200 W, 33 ± 3 kHz, 1 h) followed by addition of 2 ml of KOH solution. The yellow–brown suspension turned in to black color, after it was heated for few minutes at $80^0$C. The suspension was then allowed to cool to room temperature decanted and the residue was dried in an air oven. The sample was labelled as REGO.

### Synthesis of sulfur-doped exfoliated graphene oxide

The S-REGO sheets were synthesized by using only REGO sheets and $Na_2S$ precursors through a hydrothermal reaction at $200^0$C in one pot [15]. Firstly, without any polymers or surfactants, a homogenous GO aqueous solution (3mg $ml^{-1}$) was obtained, which was synthesized by modified Hummer's method. Then, a given amount of $Na_2S$ (0.05g, 0.1g and 0.2g $Na_2S$) was introduced into 80 ml of GO aqueous solution under magnetic stirring at $25^0$C for 10 min, subsequently the above solution was transferred and sealed into a Teflon-lined stainless steel autoclave (100ml), heated to $200^0$C and maintained at this temperature for 10 h to obtain a dispersion containing S-REGO sheets. After, the resulting dispersion containing S-REGO sheets was naturally cooled to room temperature, purified by filtration and washed with deionized water several times. Finally, the resulting S-REGO sheets were obtained after air drying.

### Synthesis of phosphorous-doped exfoliated graphene oxide

The P-REGO sheets were synthesized by using REGO sheets and phosphoric acid precursors [14]. We take first 2g GO in 100 ml water in one pot. Then, we take $H_3PO_4$solution of different amount(1M $H_3PO_4$ in 200ml water, 1.5M $H_3PO_4$ in 200ml water and 2M $H_3PO_4$ in 200ml water) in another pot. After stirring 15 min, we mixed both solution followed by drying at $220^0$C. The excess phosphoric acid was removed by washing the samples with hot water until the pH of the wash water become neutral. The samples were finally dried at $110^0$C and labeled as P-REGO.

### Electrode preparation

The working electrode for electrochemical testing were prepared (Figure 1) by mixing the active material with isopropyl alcohol and NAFION solution in the desired ratio, then put in the ULTRASONICATOR for 1 hr until homogenous slurry was obtained. Electrodes of 0.5x0.5 $cm^2$ (carbon paper) were made by coating the homogenous slurry, containing the active material like SGO and PGO.

**Fig 1:** Electrode Samples

## Results and Discussion

### XRD analysis

The structural information of different samples of S-RGO and P-RGO can be obtained from the XRD analysis (Figure 2). In the S-doped RGO sheets exhibit a well-defined peak at 2-theta = $24.20^0$, indicating the partial restoration of $sp^2$ carbons. As we increase the Sulfur composition from 5 at% to 10 at%, the intensity of sulfur dopant RGO peaks gets stronger. Further increase the Sulfur content, the intensity of peak stronger from first sample of 5 at% Sulfur and weaker from second sample of 10 at% Sulfur due to inter spacing doping instead of intra spacing doping and small peak at $44.20^0$ indicating from carbon composition in the sample.

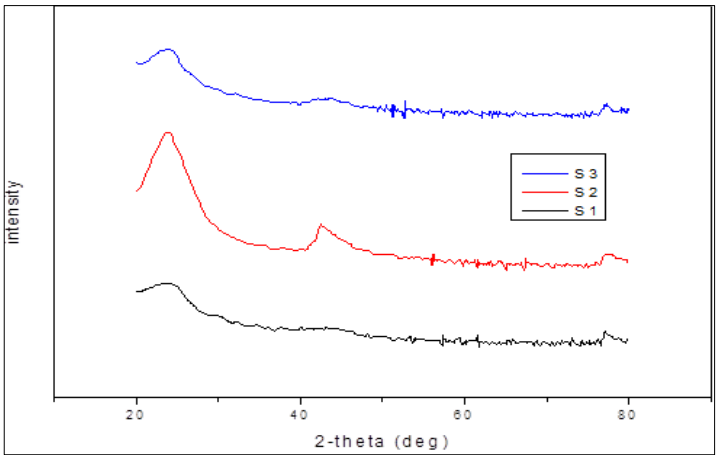


**Fig 2:** XRD patterns for S-doped RGO samples sheets (S1=5 at%, S2=10 at%, S3=20 at %)

Similarly the XRD pattern of P-doped RGO shown in Figure 3. From the figure, we observed that P-RGO sheets exhibit a well-defined peak at 2-theta = $26.30^{0,}$ which indicate the strong diffraction peak of P-dopant RGO sheets. As we increase the quantity of phosphoric acid, the intensity gets More Stronger than previous one.

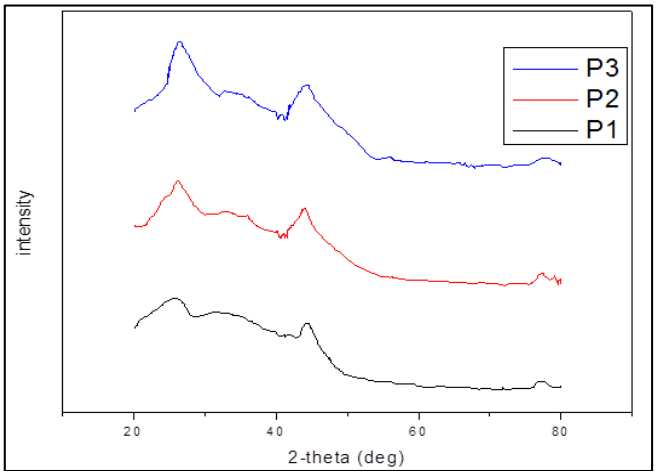


**Fig 3:** XRD patterns for P-doped RGO samples sheets (P1=1M, P2=1.5M, P3=2M of Phosphoric Acid)

**FTIR analysis**

The FTIR spectra of different sample of Sulfur- doped graphene aerogel for three different samples are shown in figure 4. The FTIR spectra of the pristine S-RGO sheets prove the presence of different functional groups, such as an O-H stretching vibration around 3450cm$^{-1}$, C-H stretching vibrations around 1450cm$^{-1}$, a C=O stretching mode at 1650cm$^{-1}$, a C=C stretching vibration around 1605cm$^{-1}$, a C-OH stretching vibration at 1200cm$^{-1}$, and small C-O stretching mode at 1020cm$^{-1}$, large -C=S stretching vibration at 1300cm$^{-1}$ and small –C-S stretching vibration at 900cm$^{-1}$. In addition, the relative intensities of O-H, C=O, C-H, C-OH, and C-O are greatly reduced from sample S1 to S3 sheets, but S2 shows the more reduction of peaks comparison to other S-doped sample, it implying that the degree of $sp^2$ domains in the S2 sheets appears to be increased comparison to other S-doped sample.

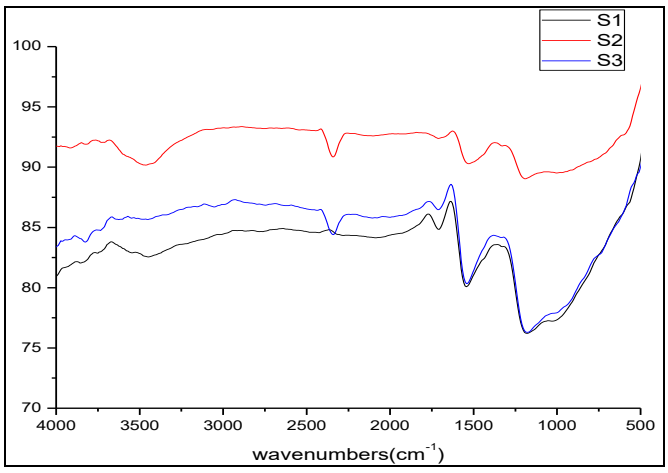


**Fig 4:** FTIR pattern of S-RGO Sheets (S1=5 at%, S2=10 at%, S3=20 at %)

Similarly, the FTIR spectra of P-RGO samples are shown in figure 5. From which it can be seen that there exists a wide absorption band at 3300-3600cm$^{-1}$ as we increase the amount of phosphoric acid due to O-H stretching mode of hydroxyl groups and absorbed water. The spectra shows a strong band at 1650-1550 cm$^{-1}$ due to aromatic ring stretching vibrations (C=C) enhanced by polar functional groups. The change in the intensity of this band parallels the phosphorous and oxygen contents of the samples. Bands at 1350-1100 cm$^{-1}$ have been assigned to C-O stretching in acids, alcohols, phenols, ethers and esters. The peaks at 1100-1050 cm$^{-1}$ may be ascribed to ionized linkage $P^{+}$-$O^{-}$ in acid phosphate esters and to symmetrical vibrations in a chain of P-O-P (polyphosphate). The shoulder at 1000-950 cm$^{-1}$ may be due to asymmetric stretching, P-O stretching, P-OH stretching, P-O-P asymmetric stretching in polyphosphate and symmetrical stretching of $PO_2$ and $PO_3$ in phosphate graphene complexes. The intensity of O-H, C=C and C-O greatly reduced as we increase the amount of phosphoric acid from P1 to P3.

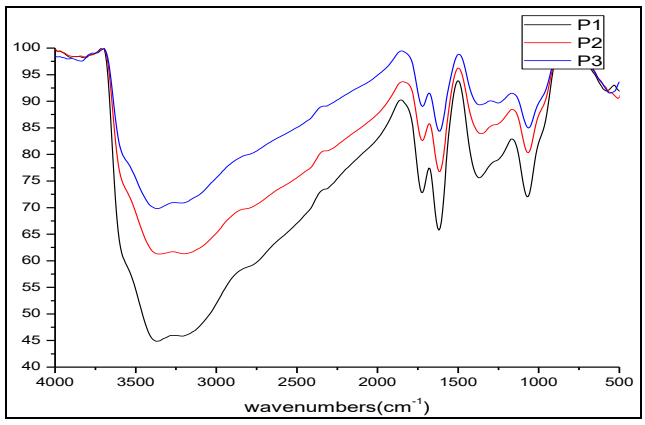


**Fig 5:** FTIR pattern of P-RGO sheets (P1=1M, P2=1.5M, P3=2M of Phosphoric Acid)

**HR - SEM analysis**

We have shown here HR-SEM images (Model, SUPRA 40, (Zeiss) of three different samples prepared of S-RGO and P-RGO in which we doped Sulfur and Phosphorous in increasing amount. The surfaces of the particles are Nano porous, irregular and contain a number of heterogeneous holes on which Sulfur and Phosphorous atoms occupied the vacancies. This has been very clear from the figures that amount of doped Sulfur and Phosphorous has been increased from figure no. 6 to figure no. 8. In figure, the amount of guest Sulfur and Phosphorous atoms over the graphene sheets have been increased by a certain amount.

**S-doped GO**

Subsequently, monolayer or few-layer of S-RGO sheets will be formed by using $Na_2S$ as a sulfur doped source and reducing agent through a hydrothermal reaction process at 200 $^{0}$C in one pot (Figure 6). The detailed nano scale morphologies of S-RGO sheets are shown in the SEM image. The low magnification SEM image of different S-doped RGO sheets shows some distinct folds and wrinkling, as we increase the sulfur content the more distinct folds and wrinkling, because the functional groups and the contraction induced by sulfur doping disrupt the original conjugation and some oxygen containing functional groups on the surfaces of S-RGO sheets, resulting in more folds and distortions on the surfaces of the S-doped RGO sheets. Furthermore, from the observation of SEM images, the surface of the S-doped RGO sheets also shown more waviness and looks like a loosely attacked gauze, some different from the low sulfur content sheets of S-RGO.

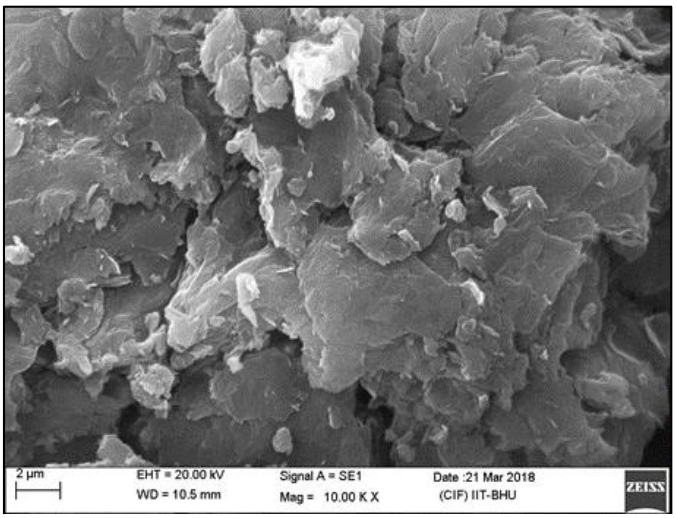


Sample S1 (5wt%Na2S)

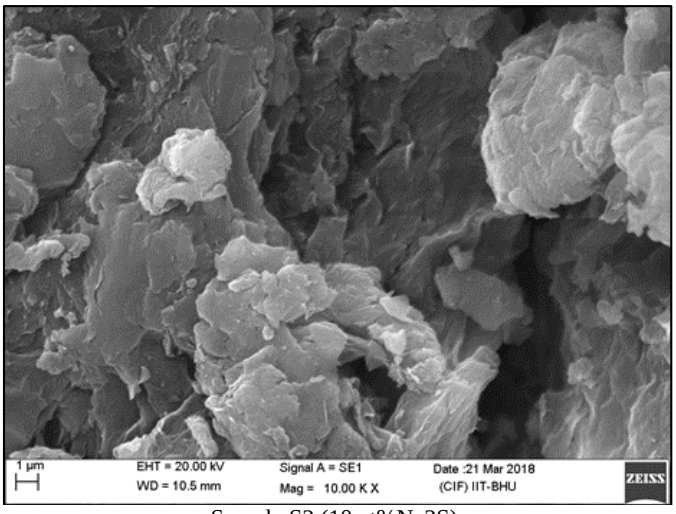


Sample S2 (10wt%Na2S)

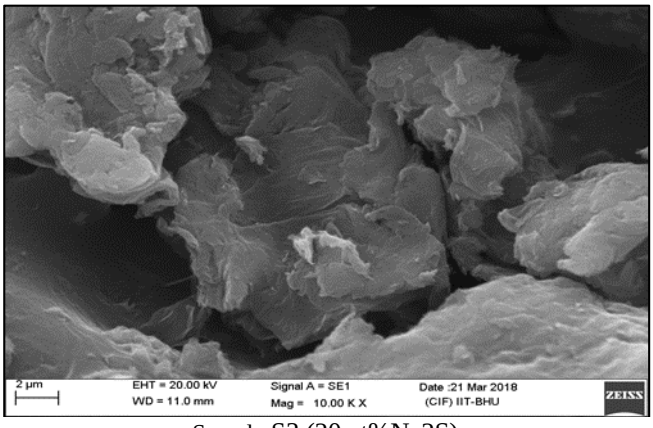


Sample S3 (20wt%Na2S)

**Fig 6:** SEM images of S-RGO sheets (S1=5 at%, S2=10 at%, S3=20 at %)

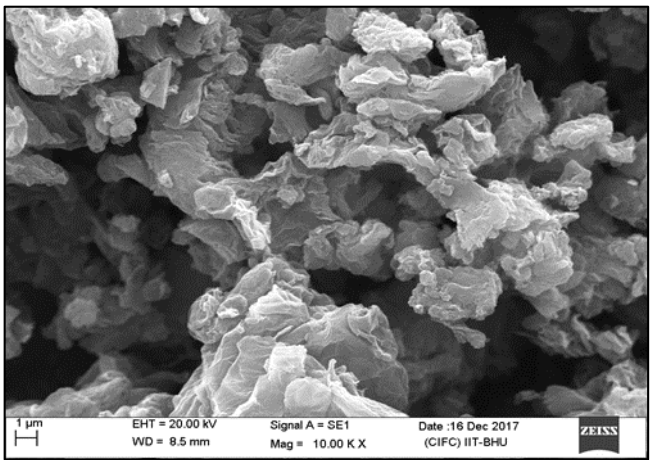


Sample P1 (1M H3PO4 in 200ml water)

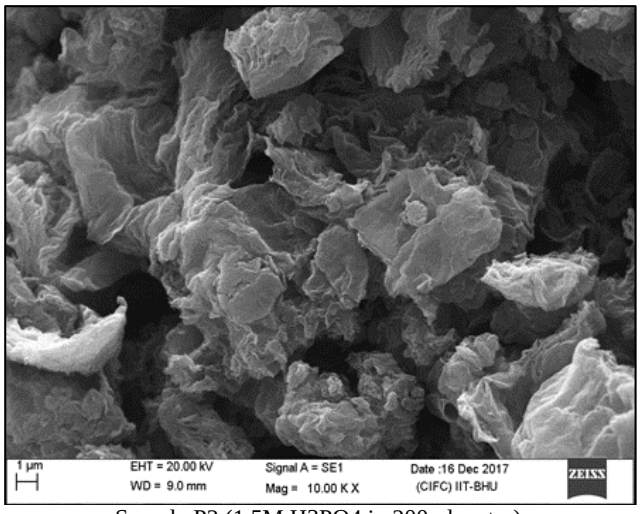


Sample P2 (1.5M H3PO4 in 200ml water)

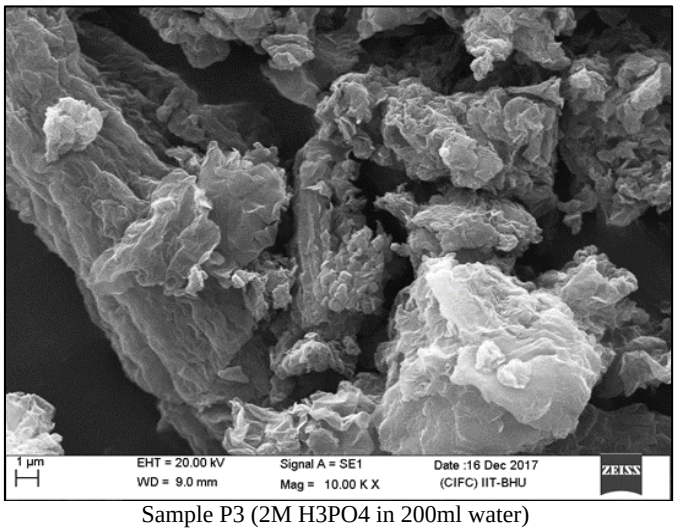


Sample P3 (2M H3PO4 in 200ml water)

**Fig 7:** SEM images of P-RGO sheets (P1=1M, P2=1.5M, P3=2M of Phosphoric Acid)

**P-doped GO**

Similarly, monolayer or few- layer P-RGO sheets will be formed by using Phosphoric Acid ($H_3PO_4$) as a phosphorous dopant source (Figure 7). The surface morphology of the P-doped RGO showed in SEM images of different P-doped RGO samples. The SEM images of all samples show transparent and rippled silk waves with many wrinkles probably due to the oxygen functional groups and contraction induced by phosphorous doping. As we increase the amount of phosphoric acid, more folds as well as wrinkles will be formed.

**Electrochemical behavior of the super capacitor**

**Cyclic voltammetry**

The figure shows the cyclic voltammetry of all the prepared capacitors at a scan rate 20 mv $s^{-1}$ (Figure 8 and 9) It is very clear from the figure that the presence of functional groups and heteroatom contribute in the form of pseudo capacitance to the specific capacitance. The more spreading of the figure shows the more capacitance, low contact resistance and clear proof of well develop capacitance properties even at higher

scan rates. The specific capacitance of the as prepared electrodes were estimated from the following equation.

$$C_s = I / v\ m\ (Fg^{-1})$$

Where $C_s$, I, v and m are the specific capacitance ($Fg^{-1}$), current (A), scan rate ($mV\ s^{-1}$) and mass of the active material (g) respectively.

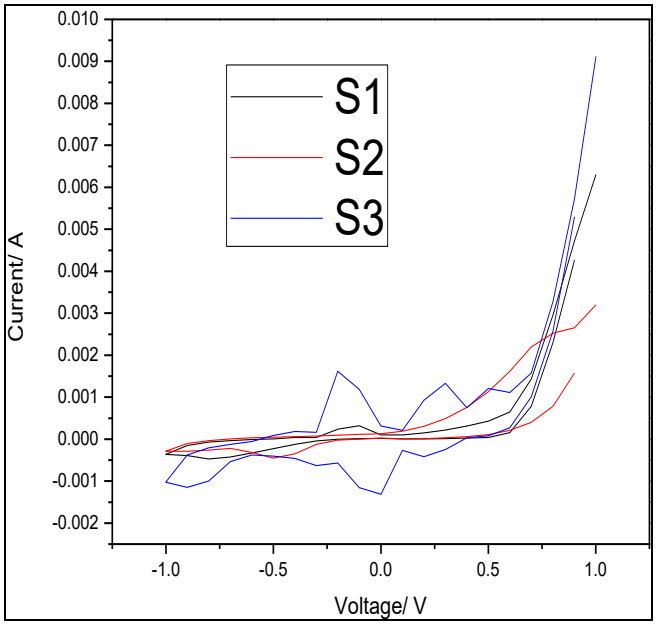


**Fig 8:** Cyclic voltammetry of different S-doped GA with scan rate 20mV $s^{-1}$ with 1M KOH as a electrolyte (S1=5 at%, S2=10 at%, S3=20 at %)

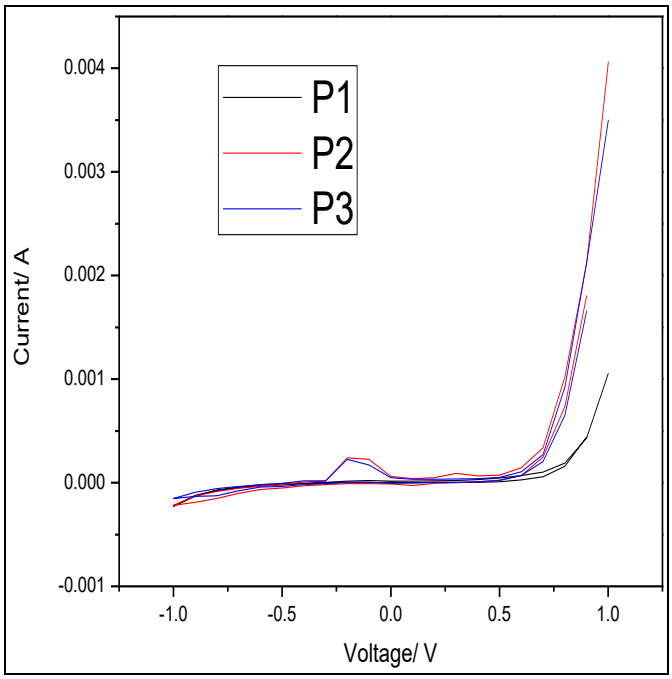


**Fig 9:** Cyclic voltammetry of different P-doped GA with scan rate 20mV $s^{-1}$ with 1M KOH as a electrolyte (P1=1M, P2=1.5M, P3=2M of Phosphoric Acid)

The variation of specific capacitance with increase in the scan rate is given in below figure 10. Significantly higher capacitance values are obtained from S doped graphene than P doped graphene. The specific capacitance values of the Sulfur doped graphene aerogel and Phosphorous doped graphene aerogel are 750.75 $Fg^{-1}$ and 360.75$Fg^{-1}$ respectively at scan rate of 20mV $s^{-1}$. The high specific capacitance by SGO may be attributed to the increased pseudo capacitance due to Sulfur doping and increased conducting network due to the reduction of graphene oxides.

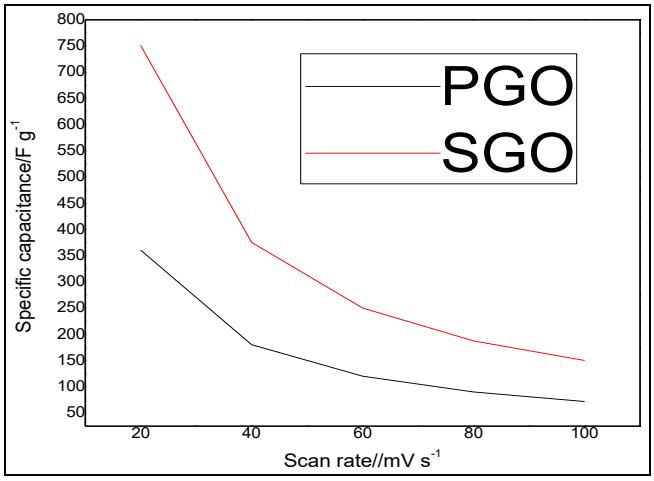


**Fig 10:** Decay of specific capacitance with various scan rates

**EIS Analysis**

EIS Analysis is done here for estimating solution resistance ($R_e$) and charge transfer or polarization resistance ($R_{ct}$) in Figure 11 and 12. In case of Sulfur doping RGO, as we increase the sulfur composition, the solution resistance ($R_e$) of samples shifted towards origin in X-axis, it shows that increasing the sulfur composition decreasing the solution resistance and less diameter semicircle will formed then shifted parallel to Y-axis, shows the less charge transfer resistance ($R_{CT}$). So, the increasing amount of sulfur shows the less solution resistance as well as charge transfer resistance. But in case of phosphorous doped RGO, the solution as well as charge transfer resistance will be large as compare to sulfur doped RGO. So, we can say that S-doped RGO is better than P-doped RGO from the point of EIS analysis.

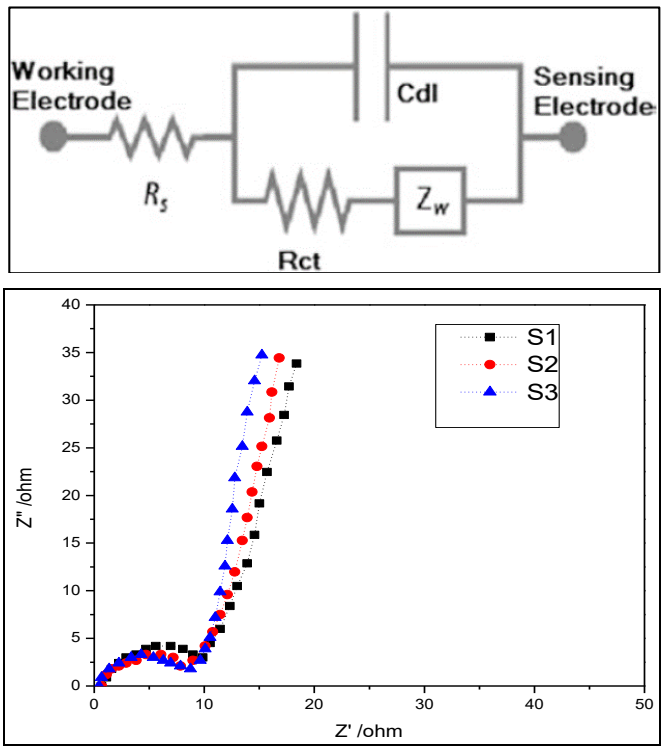


**Fig 11:** Impedance comparison of Sulfur-doped RGO samples (S1=5 at%, S2=10 at%, S3=20 at %)

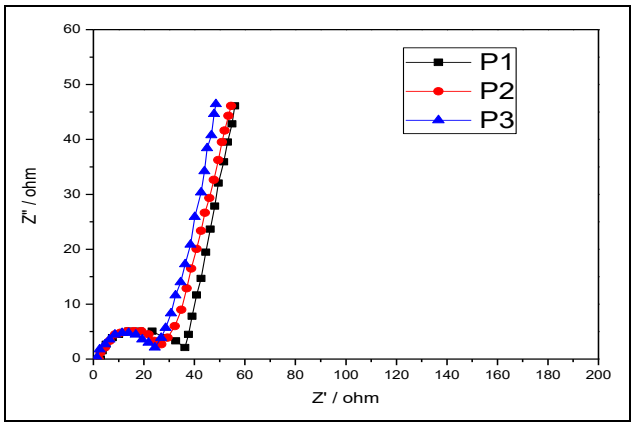


**Fig 12:** Impedance comparison of phosphorous-doped RGO samples (P1=1M, P2=1.5M, P3=2M of Phosphoric Acid)

**Galvanostatic charge-discharge profiles**

Galvanostatic charge-discharge curves of super capacitor electrodes carried at a constant current density of 10mA $cm^{-2}$ are shown in figures 13 and 14. As we increase the composition of Sulfur and Phosphorous, the voltage inside the super capacitor will be increase in small amount and also increase the charge & discharge time. The value of specific capacitance (C) is greater in Sulfur doped RGO as compare to Phosphorous doped RGO. But from the graph we can see that charge storage time is greater in S-doped RGO comparison to P-doped RGO.

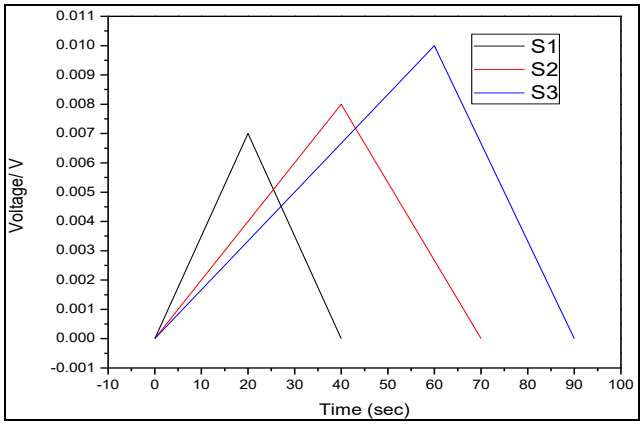


**Fig 13:** Charge-Discharge Profiles of Sulfur-doped RGO (S1=5 at%, S2=10 at%, S3=20 at %)

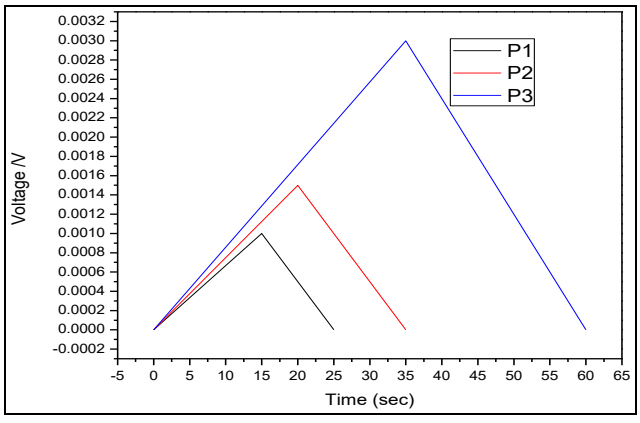


**Fig 14:** Charge-Discharge Profiles of Phosphorous-doped RGO (P1=1M, P2=1.5M, P3=2M of Phosphoric Acid)

## Conclusion

In this study, we demonstrate a facile synthesis of S-doped RGO sheets with good electrical properties as compare to P-doped RGO by using only GO sheets using Hummer's method and $Na_2S$ as precursors through a mild hydrothermal reactions process at 200 $^0$C in one pot, without any polymers or surfactants. Graphene doped with Sulfur exhibit enhanced capacitive performance in aqueous electrolyte as compare to Phosphorous doped due to increased pseudo capacitance and good electrical conducting network in the electrode structure. The S-RGO sheets can normally be fabricated on a large scale, when the atomic percentage of S reaches a maximum of 20 at%. The current value is much higher than that of P-doped RGO under the same test conditions. Super capacitor fabricated using Sulfur and Phosphorous doped RGO showed a high specific capacitance of 750.75 $Fg^{-1}$ and 360.75 $Fg^{-1}$ respectively. During the hydrothermal reaction process, the introduced $Na_2S$ can act as not only a sulfur dopant, but also as a reducing agent in the formation of S-RGO sheets. The synergistic effects of a sulfur dopant, Phosphorous dopant and reducing agent dramatically improve the electrical conductivities of the resulting S-RGO sheets as we increase the amount of Sulfur and Phosphorous. These highly conductive S-RGO sheets offer many promising technological applications such as efficient metal free electro catalysts in oxygen reduction reactions in fuel cells and as super capacitor electrode materials for high performance Li-ion batteries. Further work is in progress.

## References


1. Min Z, Wen-Long W, Xue-Dong B. Preparing three-dimensional graphene architectures: review of recent developments. Chin. Phys. 2013; 22: 98-105.
2. Xu Y, Sheng K, Li C, Shi G. Self-assembled graphene hydrogel via a one-step hydrothermal process. *ACS* Nano. 2010; 4(7):4324-4330.
3. Zhu C, Liu T, Qian F, Han TYJ, Duoss EB, Kuntz JD, et al. Super capacitors based on three-dimensional hierarchical graphene aerogels with periodic macropores. Nano letters. 2016; 16(6):3448-3456.
4. Si W, Wu X, Zhou J, Guo F, Zhuo S, Cui H. et al. Reduced graphene oxide aerogel with high-rate supercapacitive performance in aqueous electrolytes. Nanoscale Res. Lett. 2013; 8:247.
5. Erickson K, Erni R, Lee Z, Alem N, Gannett W, Zettl, A. Determination of the local chemical structure of graphene oxide and reduced graphene oxide. Advanced Materials. 2010; 22(40):4467-4472.
6. Li C, Shi G. Three-dimensional graphene architectures. Nanoscale. 2012; 4:5549-5563.
7. Li W, Wang J, Ren, J, Qu, X. 3D graphene oxide–polymer hydrogel: near-infrared light-triggered active scaffold for reversible cell capture and on-demand release. Adv. Mater. 2013; 25:6737–6743.
8. Yang Z, Yao Z, Li G, Fang G, Nie H, Liu Z. Sulfur-doped graphene as an efficient metal-free cathode catalyst for oxygen reduction. ACS nano. 2011, 2011; 6(1):205-211.
9. Jiang Y, Lu M, Ling X, Jiao Z, Chen L, Chen L. et al. One-step hydrothermal synthesis of three-dimensional porous graphene aerogels/sulfur nanocrystals for lithium–sulfur batteries. Journal of Alloys and Compounds. 2015; 645:509-516.
10. Cai ZX, Song XH, Chen YY, Wang YR, Chen X. 3D nitrogen-doped graphene aerogel: A low-cost, facile prepared direct electrode for H2O2 sensing. Sensors and Actuators B: Chemical. 2016; 222:567-573.
11. Novoselov KS, Geim AK, Morozov S, Jiang D, Katsnelson M, Grigorieva I. Two-dimensional gas of

massless Dirac fermions in graphene. *Nature*. 2005; 438(7065), 197.
12. Jiang H, Lee PS, Li C. 3D carbon based nanostructures for advanced supercapacitors. Energy Environ. Sci. 2013; 6:41-53.
13. Kuang J, Liu L, Gao Y, Zhou D, Chen Z, Han B, Zhang Z. A hierarchically structured graphene foam and its potential as a large-scale strain-gauge sensor. Nanoscale. 2013; 5(24):12171-12177.
14. Karthika P, Rajalakshmi N, Dhathathreyan KS. Phosphorus-doped exfoliated graphene for supercapacitor electrodes. Journal of nanoscience and nanotechnology. 2013; 13(3):1746-1751.
15. Tian Z, Li J, Zhu G, Lu J, Wang Y, Shi Z, *et al*. synthesis of highly conductive sulfur-doped reduced graphene oxide sheets. Physical Chemistry Chemical Physics. 2016; 18(2):1125-1130.